

An efficient image encryption scheme based on ordered quasi-resonant Rossby/drift wave triads and Mordell elliptic curves

Ikram Ullah¹, Umar Hayat¹ and Miguel D. Bustamante^{2,*} 

¹ Department of Mathematics, Quaid-i-Azam University, Islamabad, Pakistan

² School of Mathematics and Statistics, University College Dublin, Belfield, Dublin 4, Ireland

* Correspondence: miguel.bustamante@ucd.ie

Abstract: We propose an image encryption scheme based on quasi-resonant Rossby/drift wave triads (related to elliptic surfaces) and Mordell elliptic curves (MECs). By defining a total order on quasi-resonant triads, at a first stage we construct quasi-resonant triads using auxiliary parameters of elliptic surfaces in order to generate pseudo-random numbers. At a second stage, we employ a MEC to construct a dynamic substitution box (S-box) for the plain-image. The generated pseudo-random numbers and S-box are used respectively to provide diffusion and confusion in the tested image. We test the proposed scheme against well-known attacks by encrypting all gray images taken from the USC-SIPI image database. Our experimental results indicate the high security of the newly developed scheme. Finally, via extensive comparisons we show that the new scheme outperforms other popular schemes.

Keywords: Quasi-resonant Rossby/drift wave triads; Mordell elliptic curve; Pseudo-random numbers; Substitution box

1. Introduction

The exchange of confidential images via internet is usual in today's life, even though the internet is an open source that is unsafe and unauthorised persons can steal useful or sensitive information. Therefore it is essential to be able to share images in a secure way. This goal is achieved by cryptography. Traditional cryptographic techniques such as data encryption standard (DES) and advanced encryption standard (AES) are not suitable for image transmission because image pixels are usually highly correlated [1,2]. In contrast, DES and AES are ideal techniques for text encryption [3], so researchers are trying to develop such techniques to meet the demand for reliable image delivery.

A number of image encryption schemes have been developed using different approaches [4–12]. One of the dominant trends in encryption techniques is the chaos based encryption [13–18]. The reason is that the chaos based encryption schemes are highly sensitive to the initial parameters. The chaos based algorithms normally use pseudo-random numbers and substitution boxes (S-boxes) to create confusion and diffusion [19,20]. “Confusion” means to hide the relation between input image, secret keys and the corresponding cipher-image, and “diffusion” means to alter the value of each pixel in an input image [1]. Cheng et al. [19] proposed an image encryption algorithm based on pseudo-random numbers and AES S-box. The pseudo-random numbers are generated using AES S-box and chaotic tent maps. The scheme is optimised by combining the permutation and diffusion phases, but the image is encrypted in rounds which is time consuming. Belazi et al. [20] suggested an image encryption algorithm using a new chaotic map and logistic map. The new chaotic map is used to generate a sequence of pseudo-random numbers for a masking phase. Then eight dynamic S-boxes are generated. The masked image is substituted in blocks via aforementioned S-boxes. The substituted image is again masked by another pseudo-random sequence

generated by the logistic map. Finally the encrypted image is obtained by permuting the masked image. The permutation is done by a sequence generated by the map function. This algorithm fulfils the security analysis but performs slowly due to the four cryptographic phases. In [21] an image encryption method based on chaotic maps and dynamic S-boxes is proposed. The chaotic maps are used to generate the pseudo-random sequences and S-boxes. To break the correlation, pixels of an input image are permuted by the pseudo-random sequences. In a second phase the permuted image is decomposed into blocks. Then blocks are encrypted by the generated S-boxes to get the cipher-image. From histogram analysis it follows that the suggested technique generates cipher-images with a nonuniform distribution.

Similar to the chaotic maps, Elliptic Curves (ECs) are sensitive to input parameters, but EC based cryptosystems are more secure than those of chaos [22]. Toughi et al. [23] developed a hybrid encryption algorithm using elliptic curve cryptography (ECC) and AES. The points of an EC are used to generate pseudo-random numbers and keys for encryption are acquired by applying AES to the pseudo-random numbers. The proposed algorithm gets the promising security but pseudo-random numbers are generated via the group law, which is time consuming. In [3] a cyclic EC and a chaotic map are combined to design an encryption algorithm. The developed scheme overcomes the drawbacks of small key space but is unsafe to the known-plaintext/chosen-plaintext attack [24]. Similarly Hayat et al. [25] proposed an EC based encryption technique. The stated scheme generates pseudo-random numbers and dynamic S-boxes in two phases, where the construction of S-box is not guaranteed for each input EC. Therefore, changing of ECs to generate an S-box is a time-consuming work. Furthermore, the generation of ECs for each input image makes it insufficient.

Based on the above discussion, we propose an improved image encryption algorithm, based on quasi-resonant Rossby/drift wave triads [26,27] (triads, for short) and Mordell Elliptic Curves (MECs). The triads are utilised in the generation of pseudo-random numbers and MECs are employed to create dynamic S-boxes using the technique introduced in [28]. The proposed scheme is novel in that it introduces the technique of pseudo-random numbers generation using triads, which is faster than generating pseudo-random numbers by ECs. Moreover, the scheme does not require to separately generate triads for each input image of the same size. In the present scheme MECs are used opposite to [25] in the sense that now, for each input image, the generation of a dynamic S-box is guaranteed [29]. Finally, extensive performance analyses and comparisons reveal the efficiency of the proposed scheme.

This paper is organised as follows. Preliminaries are described in Section 2. In Section 3, the proposed encryption algorithm is explained in detail. Section 4 provides the experimental results of the newly developed scheme. A comparison is drawn in Section 5 between the proposed method and existing popular schemes. Lastly, conclusions are presented in Section 6.

2. Preliminaries

Barotropic vorticity equation: The barotropic vorticity equation (in the so-called β -plane approximation) is a partial differential equation of the form

$$\frac{\partial}{\partial t}(\nabla^2\psi - F\psi) + \left(\frac{\partial\psi}{\partial x} \frac{\partial\nabla^2\psi}{\partial y} - \frac{\partial\psi}{\partial y} \frac{\partial\nabla^2\psi}{\partial x} \right) + \gamma \frac{\partial\psi}{\partial x} = 0, \quad (1)$$

where $\psi(x, y, t) \in \mathbb{R}$ represents the stream function, γ is a real constant and F is a non-negative real constant. We assume periodic boundary conditions: $\psi(x + 2\pi, y, t) = \psi(x, y + 2\pi, t) = \psi(x, y, t)$ for all $x, y, t \in \mathbb{R}$. In literature Eq. (1) is also known as the Charney-Hasegawa-Mima equation (CHM) [30–34]. This equation accepts many special solutions, including travelling wave solutions. Of central importance is the so-called Rossby wave, which is a solution of both the linearised form and the whole (nonlinear) form of Eq. (1). This solution is given explicitly by the parameterised function $\psi_{(k,l)}(x, y, t) = e^{i(kx+ly-\omega(k,l)t)}$,

where $\omega(k, l) = -\frac{\gamma k}{k^2 + l^2 + F}$ is called the angular frequency and $(k, l) \in \mathbb{Z}^2$ is called the wave vector. For simplicity we take $\gamma = -1$ and $F = 0$ in what follows [26,27].

Resonant triad, quasi-resonant triad and detuning level: A linear combination of Rossby waves parameterised by wave vectors that are not collinear, is again a solution of the linearised form of Eq. (1), but not a solution of the whole equation. However, to the lowest order of nonlinearity in Eq. (1), approximate solutions known as resonant triad solutions can be constructed via linear combinations. Any set of three wave vectors (k_1, l_1) , (k_2, l_2) and (k_3, l_3) satisfying the equations:

$$k_1 + k_2 = k_3, l_1 + l_2 = l_3 \quad \text{and} \quad \omega_1 + \omega_2 = \omega_3, \quad (2)$$

for $\omega_i = \omega(k_i, l_i)$, $i = 1, 2, 3$ is called a resonant triad. If the equation $\omega_1 + \omega_2 = \omega_3$ is replaced by the inequality $|\omega_1 + \omega_2 - \omega_3| \leq \delta^{-1}$, for a large positive number δ , then the triad becomes a quasi-resonant triad and δ^{-1} is known as the detuning level of the quasi-resonant triad. For simplicity, in what follows we call a quasi-resonant triad simply a triad and denote it by Δ . Finally, to avoid over-counting of triads we will impose the condition $k_3 > 0$.

Rational transformation: In [26] wave vectors are explicitly expressed in terms of rational variables X, Y and D as follows:

$$\frac{k_1}{k_3} = \frac{X}{Y^2 + D^2}, \quad \frac{l_1}{k_3} = \left(\frac{X}{Y}\right) \left(1 - \frac{D}{Y^2 + D^2}\right), \quad \frac{l_3}{k_3} = \frac{D - 1}{Y}. \quad (3)$$

In the case $F = 0$ the rational variables X, Y, D lie on an elliptic surface. The transformation is bijective and its inverse mapping is given by:

$$X = \frac{k_3(k_1^2 + l_1^2)}{k_1(k_3^2 + l_3^2)}, \quad Y = \frac{k_3(k_3 l_1 - k_1 l_3)}{k_1(k_3^2 + l_3^2)}, \quad D = \frac{k_3(k_3 k_1 - l_1 l_3)}{k_1(k_3^2 + l_3^2)}. \quad (4)$$

New parameterisation: In [35], Kopp parameterised the resonant triads and in terms of parameters u and t it follows by [35, Eq. (1.22)] that:

$$\frac{k_1}{k_3} = (t^2 + u^2)(t^2 - 2u + u^2)/(1 - 2u), \quad (5)$$

$$\frac{l_3}{k_3} = (u(2u - 1) + (t^2 + u^2)(t^2 - 2u + u^2))/(t(1 - 2u)), \quad (6)$$

$$\frac{l_1}{k_3} = (t^2 + u^2)((2u - 1) + u(t^2 - 2u + u^2))/(t(1 - 2u)). \quad (7)$$

In 2019, Hayat et al. [27] found a new parameterisation of X, Y and D in terms of auxiliary parameters a, b and hence $\frac{k_1}{k_3}, \frac{l_3}{k_3}$ and $\frac{l_1}{k_3}$ are given by:

$$\frac{k_1}{k_3} = \frac{(a^2 + b(2 - 3b) + 1)^3}{(a^2 - 3b^2 - 2b + 1)(2(11 - 3a^2)b^2 + (a^2 + 1)^2 - 16ab + 9b^4)}, \quad (8)$$

$$\frac{l_3}{k_3} = \frac{6(a^2 + a - 1)b^2 - (a + 1)^2(a^2 + 1) + 4ab - 9b^4}{(a^2 - 3b^2 - 1)(a^2 - 3b^2 - 2b + 1)}, \quad (9)$$

$$\frac{l_1}{k_3} = \frac{(a^2 + b(2 - 3b) + 1)}{(a^2 - 3b^2 - 1)(a^2 - 3b^2 - 2b + 1)(2(11 - 2a^2)b^2 + (a^2 + 1)^2 - 16ab + 9b^4) \times [a^6 + 2a^5 + a^4(-9b^2 - 6b + 3) - 4a^3(3b^2 + 2b - 1) + 3a^2(3b^2 + 2b - 1)^2 + 2a(9b^4 + 12b^3 + 14b^2 - 4b + 1) - (3b^2 + 1)^2(3b^2 + 6b - 1)]}. \quad (10)$$

Elliptic curve: Let \mathbb{F}_p be a finite field for any prime p , then an EC E_p over \mathbb{F}_p is defined by

$$y^2 \equiv x^3 + bx + c \pmod{p}, \quad (11)$$

where $b, c \in \mathbb{F}_p$. The integers b, c and p are called parameters of an EC. The number of all $(x, y) \in \mathbb{F}_p^2$ satisfying the congruence (11) is denoted by $\#E_p$. For $b = 0$, the type of ECs is known as Mordell elliptic curve (MEC). If points on E_p are ordered according to some total order \prec then E_p is said to be an ordered EC. Recall that total order is a binary relation which possesses the reflexive, antisymmetric and transitive properties. Azam et al. [28] introduced a total order known as a natural ordering on MECs given by

$$(x_1, y_1) \prec (x_2, y_2) \Leftrightarrow \begin{cases} \text{either } x_1 < x_2, \text{ or} \\ x_1 = x_2 \text{ and } y_1 < y_2, \end{cases}$$

and generated efficient S-boxes using the aforesaid ordering. We will use natural ordering to generate S-boxes. Thus from here on E_p stands for a naturally ordered MEC unless it is specified otherwise.

3. The Proposed encryption scheme

The proposed encryption scheme is based on pseudo-random numbers and S-boxes. The pseudo-random numbers are generated using quasi-resonant triads. To get an appropriate level of diffusion we need to properly order the Δ s. For this purpose we define a binary relation \lesssim as follows.

3.1. Ordering on quasi-resonant triads

Let Δ, Δ' represent the triads $(k_i, l_i), (k'_i, l'_i), i = 1, 2, 3$ respectively, then

$$\Delta \lesssim \Delta' \Leftrightarrow \begin{cases} \text{either } a < a', \text{ or} \\ a = a' \text{ and } b < b', \text{ or} \\ a = a', b = b' \text{ and } k_3 \leq k'_3, \end{cases}$$

where a, b and a', b' are the corresponding auxiliary parameters of Δ and Δ' respectively.

Lemma 1. *If T denotes the set of Δ s in a box of size L , then \lesssim is a total order on T .*

Proof. The reflexivity of \lesssim follows from $a = a, b = b$ and $k_3 = k_3$ and hence $\Delta \lesssim \Delta$. As for antisymmetry we suppose $\Delta \lesssim \Delta'$ and $\Delta' \lesssim \Delta$. Then, by definition $a \leq a'$ and $a' \leq a$, which imply $a = a'$. So we are left with two results: $b \leq b'$ and $b' \leq b$, which imply $b = b'$. Thus, we obtain the results $k_3 \leq k'_3$ and $k'_3 \leq k_3$, which ultimately give $k_3 = k'_3$. Solving Eqs. (8)–(10) for the obtained values we get $k_1 = k'_1, l_3 = l'_3$ and from Eq. (2) it follows that $l_2 = l'_2$. Consequently $\Delta = \Delta'$ and \lesssim is antisymmetric. As for transitivity, let us assume $\Delta \lesssim \Delta'$ and $\Delta' \lesssim \Delta''$. Then $a \leq a'$ and $a' \leq a''$, implying $a \leq a''$. If $a < a''$ then transitivity follows. If $a = a''$, then $a' = a''$ too. Thus, $b \leq b'$ and $b' \leq b''$, so $b \leq b''$. If $b < b''$ then transitivity follows. If $b = b''$, then $b' = b''$ too. Thus, $k_3 \leq k'_3$ and $k'_3 \leq k''_3$, implying $k_3 \leq k''_3$ and hence transitivity follows: $\Delta \lesssim \Delta''$. \square

Let T^* stand for the set of Δ s ordered with respect to the order \lesssim . The main steps of the proposed scheme are explained as follows.

3.2. Encryption

A. Public parameters: In order to exchange the useful information the sender and receiver should agree on the public parameters described as below:

- (1) Three sets: Choose three sets $\mathcal{A}_i = [A_i, B_i], i = 1, 2, 3$ of consecutive numbers with unknown step sizes, where the end points $A_i, B_i, i = 1, 2, 3$ are rational numbers.
- (2) A total order: Select a total order \prec so that the triads generated by the above mentioned sets may be arranged with respect to that order.

Suppose that P represents an image of size $m \times n$ to be encrypted, and the pixels of P are arranged in column wise linear ordering. Thus, for positive integer $i \leq mn$, $P(i)$ represents the i -th pixel value in linear ordering. Assume that S_P is the sum of all pixel values of image P . Then the proposed scheme chooses the secret keys in the following ways.

B. Secret keys: To generate confusion and diffusion in an image, the sender chooses the secret keys as follows.

- (1) Step size: Select positive integers a_i, b_i to construct the step sizes $\alpha_i = \frac{a_i}{b_i}$ of $\mathcal{A}_i, i = 1, 2$. Also choose a non-negative integer a_3 as a step size of \mathcal{A}_3 in such a way that $\prod_{i=1}^3 n_i \geq mn$, where $\#\mathcal{A}_i = n_i$ represents the number of elements in \mathcal{A}_i .
- (2) Detuning level: Fix some positive integer δ to find the detuning level δ^{-1} allowed for the triads.
- (3) Bound: Select a positive integer L such that $|k_i|, |l_i| \leq L$ for $i = 1, 2, 3$. This condition is imposed in order to bound the components of the triad wave vectors. Furthermore, choose an integer t to find $r = \lfloor S_P/t \rfloor$, where $\lfloor \cdot \rfloor$ gives the nearest integer when S_P is divided by t . The reason for choosing such a t is to generate key dependent S-boxes and the integer r is used to diffuse the components of triads.
- (4) A prime: Select a prime $p \geq 257$ such that $p \equiv 2 \pmod{3}$ as a secret key for computing $c \equiv S_P + t \pmod{p}$ to generate an S-box $\zeta_{E_p}(p, t, S_P)$ on the E_p .

The positive integers $a_1, b_1, a_2, b_2, a_3, \delta, L, S_P, t$ and p are secret keys. Here it is mentioned that the parameters $a_1, b_1, a_2, b_2, a_3, \delta$ and L are used to generate mn triads in a box of size L . The generation of triads is explained step by step in Algorithm 1. These triads along with keys S_P and t are used to generate the sequence $\beta_T^*(t, S_P)$ of pseudo-random numbers.

Thus Δ_j represents the j -th triad in ordered set T^* . Moreover, $(k_{ji}, l_{ji}), i = 1, 2, 3$ are the components of Δ_j . In Algorithm 2, the generation of $\beta_T^*(t, S_P)$ is explained.

The proposed sequence $\beta_T^*(t, S_P)$ is cryptographically a good source of pseudo-randomness because triads are highly sensitive to the auxiliary parameters (a, b) [27] and inverse detuning level δ . It is shown in [26] that the intricate structure of clusters formed by triads depends on the chosen δ , and the size of the clusters increases as the inverse detuning level increases. Moreover, the generation of triads is rapid due to the absence of modular operation.

C. Performing diffusion. To change the statistical properties of an input image diffusion process is performed. While performing the diffusion, the pixel values are changed using the sequence $\beta_T^*(t, S_P)$. Let

Algorithm 1: Generating Quasi-resonant triads

```

/* T is a set containing the Quasi-resonant triads, while m and n are the
dimensions of an input image.
Input : Three sets  $\mathcal{A}_i, i = 1, 2, 3$ , inverse detuning
level  $\delta$ , bound  $L$ , two positive integers  $m$  and  $n$ .
Output: Quasi-resonant triads
1  $T := \emptyset$ ;
2  $c_1 \leftarrow 0, c_2 \leftarrow 1$ ;
3 for  $a \in \mathcal{A}_1$  do
4   for  $b \in \mathcal{A}_2$  do
5      $c_1 \leftarrow c_1 + 1$ ;
6     Calculate and store the values of
        $k'_1(c_1), l'_3(c_1)$ , and  $l'_1(c_1)$  for each pair  $(a, b)$ 
       using Eqs. (8)-(10).
7   end
8 end
9 for  $c_2 \in [1, c_1]$  do
10  for  $k_3 \in \mathcal{A}_3$  do
11     $k_1 = \lfloor (k'_1(c_2) * k_3) \rfloor, l_3 = \lfloor (l'_3(c_2) * k_3) \rfloor$  and
12     $l_1 = \lfloor (l'_1(c_2) * k_3) \rfloor$ ;
13     $k_2 = k_3 - k_1, l_2 = l_3 - l_1$  and
14     $\omega_i = k_i / (k_i^2 + l_i^2), i = 1, 2, 3$ ;
15     $\omega_4 = \omega_3 - \omega_2 - \omega_1$ ;
16    if  $|\omega_4| < \delta^{-1}$  and  $0 < |k_i|, |l_i| < L, i = 1, 2, 3$ 
17    then
18       $T := T \cup \{\Delta\}$ ;
19    end
20    if  $\#T = mn$  then
21      break;
22    end
23 end
24 end
25 Sort  $T$  with respect to the ordering  $\lesssim$  to get  $T^*$ .

```

Algorithm 2: Generating the proposed pseudo-random sequence

```

Input : An ordered set  $T^*$ , an integer  $t$  and a plain-image  $P$ .
Output: Random numbers sequence  $\beta_{T^*}(t, S_P)$ .
1  $Tr(j) := |rk_{j1}| + |l_{j1}| + |k_{j2}|$ ;
2  $\beta_{T^*}(t, S_P)(j) = (Tr(j) + S_P) \pmod{256}$ ;

```

M_P denote the diffused image for a plain-image P . The proposed scheme alters the pixels of P according to the Eq. (12):

$$M_P(i) = \beta_{T^*}(t, S_P)(i) + P(i) \pmod{256}. \quad (12)$$

D. Performing confusion. Nonlinear function causes confusion in a cryptosystem, and nonlinear components are necessary for a secure data encryption scheme. The current scheme uses the dynamic S-boxes to produce the confusion in an encrypted image. If C_P stands for the encrypted image of P , then confusion is performed by the Eq. (13) as follows:

$$C_P(i) = \zeta_{E_p}(p, t, S_P)(M_P(i)). \quad (13)$$

Lemma 2. If $\#\mathcal{A}_i = n_i, i = 1, 2, 3$ and p is a prime chosen for the generation of an S-box, then the time complexity of the proposed encryption scheme is $\max\{\mathcal{O}(n_1 n_2 n_3), 256p\}$.

Proof. The computation of all possible values of k'_1, l'_3 and l'_1 in Algorithm (1) takes $\mathcal{O}(n_1 n_2)$ time. Similarly the time complexity for generating T^* is $\mathcal{O}(c_1 n_3)$ but c_1 executes $n_1 n_2$ times. Thus the time required by T^* and hence by $\beta_{T^*}(t, S_P)$ is $\mathcal{O}(n_1 n_2 n_3)$. Also Algorithm 1 in [28] shows that the proposed S-box can be constructed in $\mathcal{O}(256p)$ time. Thus the time complexity of the proposed scheme is $\max\{\mathcal{O}(n_1 n_2 n_3), 256p\}$. \square

3.3. Decryption

In our scheme the decryption process can take place by reversing the operations of the encryption process. One should know the inverse S-box $\zeta_{E_p}^{-1}(n, t, S_P)$ and the pseudo-random numbers $\beta_T^*(t, S_P)$. Assume the situation when the secret keys $a_1, b_1, a_2, b_2, a_3, \delta, L, S_P, t$ and p are transmitted by a secure channel, so that the set T is obtained using keys $a_1, b_1, a_2, b_2, a_3, \delta$ and L , and hence the S-box $\zeta_{E_p}^{-1}(p, t, S_P)$ and the pseudo-random numbers $\beta_T^*(t, S_P)$ can be computed by S_P, t and p . Finally, the receiver gets the original image P by applying the following equations:

$$M_P(i) = \zeta_{E_p}^{-1}(p, t, S_P)(C_P(i)), \quad (14)$$

$$P(i) = M_P(i) - \beta_T^*(t, S_P)(i) \pmod{256}. \quad (15)$$

4. Security analysis

In this section the security of the proposed scheme is analysed. For this purpose the current scheme is implemented on all gray images of USC-SIPI Image Database [36]. The USC-SIPI database contains images of size $m \times m$, $m = 256, 512, 1024$. Furthermore, some security analyses which are explained one by one in the associated subsections are presented. To validate the quality of the proposed scheme, the experimental results are compared with some other encryption schemes. The parameters used for the experiments are $A_1 = A_2 = -1.0541, A_3 = 401, B_1 = B_2 = -0.8514, B_3 = 691, 3036, 5071$ for $m = 256, 512, 1024$ resp., $a_1 = 2, b_1 = 1000, a_2 = 19, b_2 = 1000, a_3 = 5, \delta = 1000, t = 2, L = 90000$ and S_P varies for each P . The experiments are performed using Matlab R2016a on a personal computer with 1.8 GHz Processor and 6 GB RAM. All encrypted images of the database along with histograms are available at <https://github.com/ikram702314/Results>. Some plain-images House $_{256 \times 256}$, Stream $_{512 \times 512}$, Boat $_{512 \times 512}$ and Male $_{1024 \times 1024}$ and their cipher-images are displayed in Fig. 1.

4.1. Statistical attack

A cryptosystem is said to be secure if it has high resistance against statistical attacks. The strength of resistance against statistical attacks is measured by entropy, correlation and histogram tests. All these tests are applied to evaluate the performance of the discussed scheme.

- (1) Histogram. Histogram is a graphical way to display the frequency distribution of pixel values of an image. A secure cryptosystem generates cipher-images with uniform histograms. The histograms of the encrypted images using the proposed method are available at <https://github.com/ikram702314/Results>. However, the respective histograms for images in Fig. 1 are shown in Fig. 2. The histograms of the encrypted images are almost uniform. Moreover, the histogram of an encrypted image is totally different from that of the respective plain-image, so that it does not allow useful information to the adversaries, and the proposed algorithm can resist any statistical attack.
- (2) Entropy. Entropy is a standout feature to measure the disorder. Let I be a source of information over a set of symbols N , then entropy of I is calculated by:

$$H(I) = \sum_{i=1}^{\#N} p(I_i) \log_2 \frac{1}{p(I_i)}, \quad (16)$$

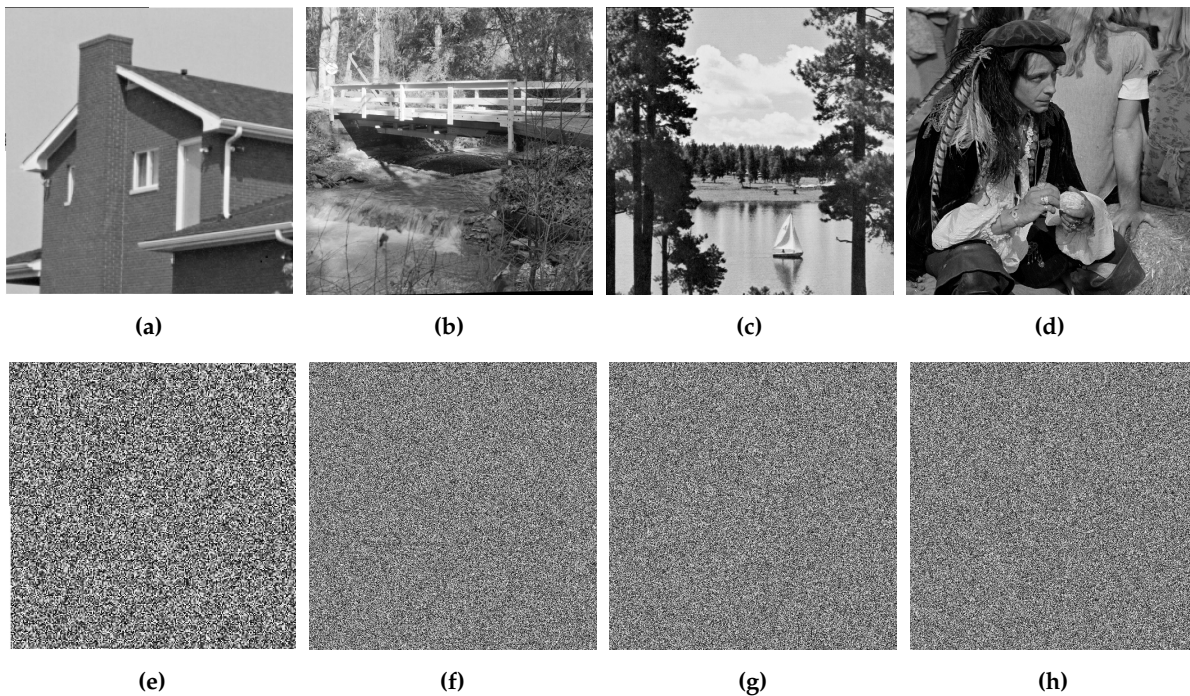


Figure 1. (a)-(d) Plain-images House, Stream, Boat and Male; (e)-(h) cipher-images of the plain-images (a)-(d), respectively.

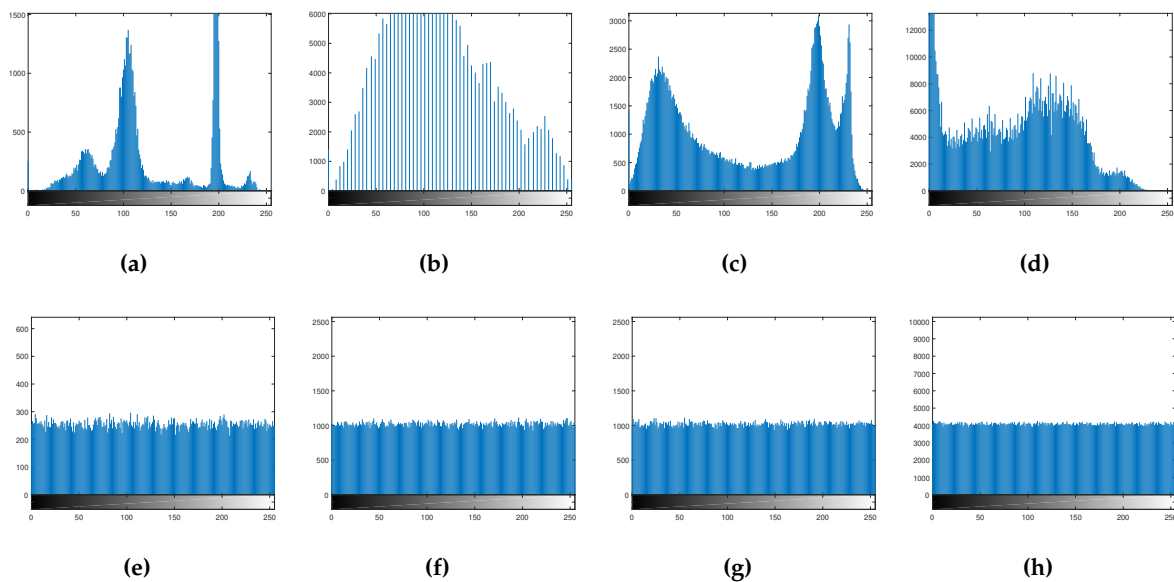


Figure 2. (a)-(d) Histograms of Fig. 1(a)-(d); (e)-(h) Histograms of Fig. 1(e)-(h).

where $p(I_i)$ is the probability of occurrence of symbol i . The ideal value of $H(I)$ is $\log_2(\#N)$, if all symbols of N occur in I with the same probability. Thus, an image I emanating 256 gray levels is absolutely pseudo-random if $H(I) = 8$. The entropy results for all images encrypted by the suggested technique are shown in Fig. 3, where the minimum, average and maximum values are 7.9966, 7.9986 and 7.9999 respectively. These results are close to 8, and hence the developed mechanism is secure against entropy attacks.

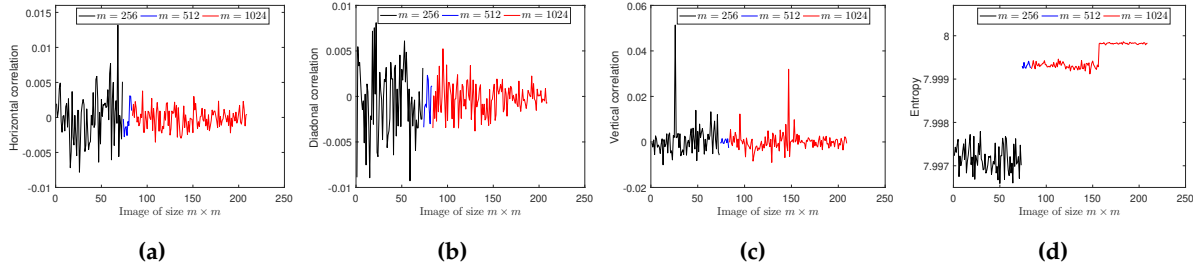


Figure 3. (a)-(c) The horizontal, diagonal and vertical correlations among pixels of each image in USC-SIPI database; (d) The entropy of each image in USC-SIPI database.

- (3) Pixel correlation. A meaningful image has strong correlation among the adjacent pixels. In fact, a good cryptosystem has the ability to break the pixel correlation and bring it close to zero. For any two gray values x and y , the pixel correlation can be computed as:

$$C_{xy} = \frac{E[(x - E[x])(y - E[y])]}{\sqrt{K[x]K[y]}}, \quad (17)$$

where $E[x]$ and $K[x]$ denote expectation and variance of x respectively. The range of C_{xy} is -1 to 1 . The gray values x and y are in low correlation if C_{xy} is close to zero. As the pixels may be adjacent in horizontal, diagonal and vertical directions, the correlation coefficients of all encrypted images along all the three directions are shown in Fig. 3, where the respective ranges of C_{xy} are $[-0.0078, 0.0131]$, $[-0.0092, 0.0080]$ and $[-0.0100, 0.0513]$. These results show that the presented method is capable of reducing the pixel correlation near to zero.

In addition, 2000 pairs of adjacent pixels of the plain-image and cipher-image of $\text{Lena}_{512 \times 512}$ are pseudo-randomly selected. Then correlation distributions of the adjacent pixels in all the three directions are shown in Fig. 4, which reveals the strong pixel correlation in the plain-image but weak pixel correlation in the cipher-image generated by the current scheme.

4.2. Differential attack

In differential attacks the opponents try to get the secret keys by studying the relation between the plain-image and cipher-image. Normally attackers encrypt two images by applying a small change to these images, then compare the properties of the corresponding cipher-images. If a minor change in original image can cause the significant change in encrypted image, then the cryptosystem has high security level. The two tests NPCR (number of pixels change rate) and UACI (unified average changing intensity) are usually used to describe the security level against differential attacks. For two plain-images P and P' different at only one pixel value, let C_P and $C_{P'}$ are the cipher-images of P and P' respectively, then NPCR and UACI are calculated as:

$$\text{NPCR} = \sum_{u=1}^m \sum_{v=1}^n \frac{\tau(u, v)}{m \times n}, \quad (18)$$

$$\text{UACI} = \sum_{u=1}^m \sum_{v=1}^n \frac{|C_P(u, v) - C_{P'}(u, v)|}{255 \times m \times n}, \quad (19)$$

where $\tau(u, v) = 0$ if $C_P(u, v) = C_{P'}(u, v)$ and $\tau(u, v) = 1$, otherwise. The ideal values of NPCR and UACI are 0.100 and 0.3333 respectively. We applied the above two tests on each image of the database

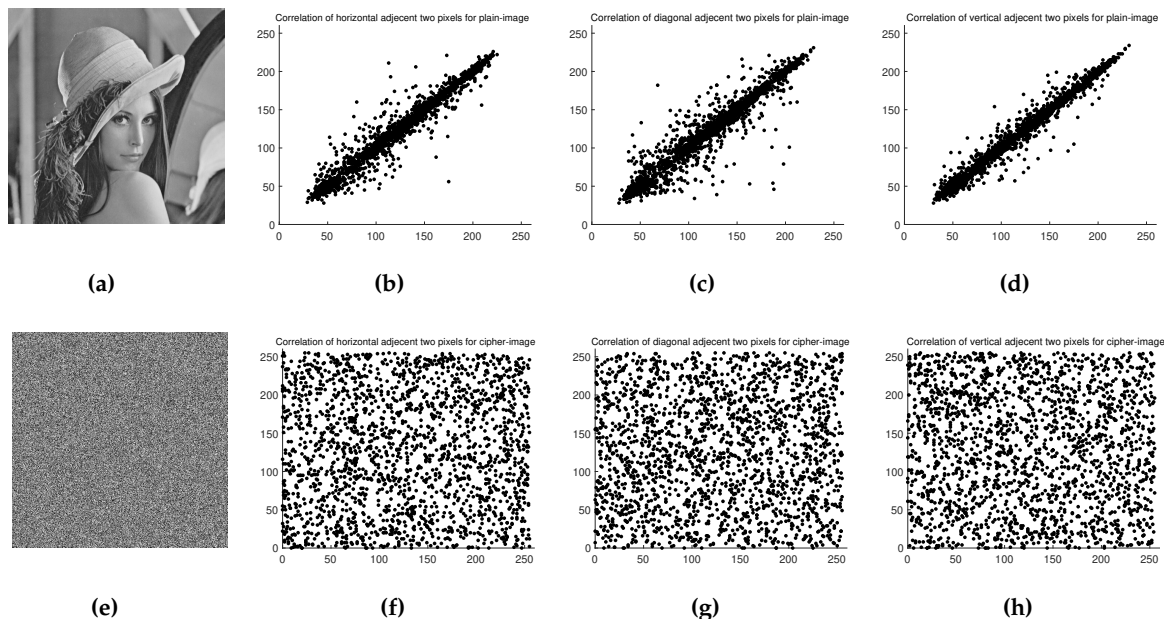


Figure 4. (b)-(d) The distribution of pixels of plane-image in horizontal, diagonal and vertical directions; (f)-(h) The distribution of pixels of cipher-image in horizontal, diagonal and vertical directions.

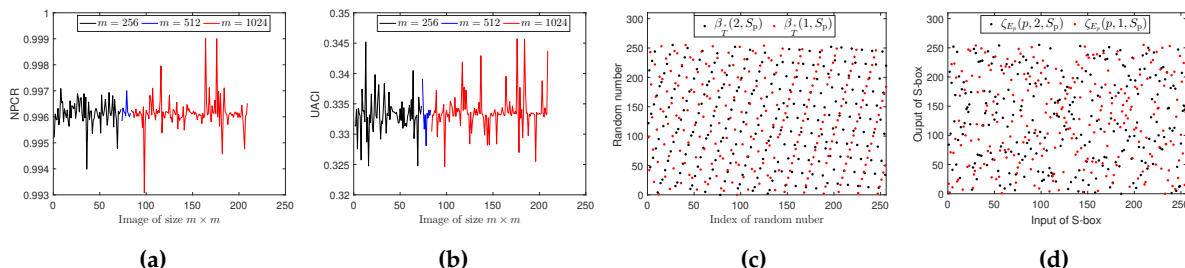


Figure 5. (a-b) The NPCR and UACI results for each image in USC-SIPI database; (c) First 256 pseudo-random numbers and (d) two S-boxes generated for $Lena_{512 \times 512}$ with a small change in an input key t .

by pseudo-randomly changing the pixel value of each image. The experimental results are shown in Fig. 5, where the average values of NPCR and UACI are 0.9961 and 0.3334 respectively. It follows from the obtained results that our scheme is capable of resisting a differential attack.

4.3. Key analysis

For a secure cryptosystem it is essential to perform well against key attacks. A cryptosystem is highly secure against key attacks if it has key sensitivity, large key space and strongly opposes the known-plaintext/chosen-plaintext attack. The proposed scheme is analysed against key attacks as follows.

- (1) Key sensitivity. Attackers usually use slightly different keys to encrypt a plain-image and then compare the obtained cipher-image with the original cipher-image to get the actual keys. Thus, high key sensitivity is essential for higher security. That is, cipher-images of a plain-image generated by slightly two different keys should be entirely different. The difference of the cipher-images is quantified by Eqs. (18) and (19). In experiments we encrypted the whole database by changing only one key, while other keys are remain unchanged. The key sensitivity results are shown in Table 1,

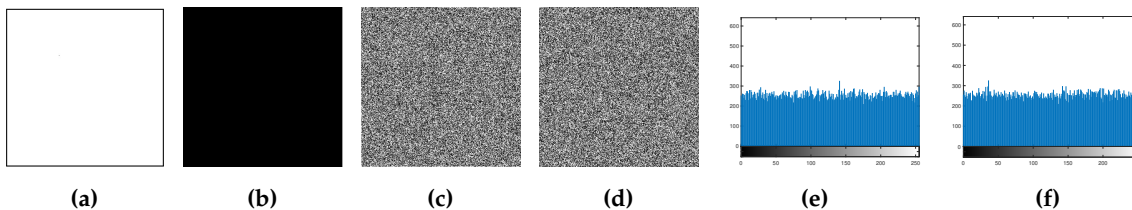


Figure 6. (a) All-white; (b) All-black; (c-d) cipher-images of (a-b); histograms of (c-d).

where the average values of NPCR and UACI are 0.9960 and 0.3341 respectively, which specify the remarkable difference in the cipher-images. Moreover, our cryptosystem is based on pseudo-random numbers and S-boxes. The sensitivity of pseudo-random numbers sequences $\beta_T^*(2, S_P)$ and $\beta_T^*(1, S_P)$ and S-boxes $\zeta_{E_p}(p, 2, S_P)$ and $\zeta_{E_p}(p, 1, S_P)$ for Lena_{512×512} is shown in Fig. 5.

Table 1. Difference between two encrypted images when key $t = 2$ is changed to $t = 1$.

Image	NPCR(%)	UACI(%)	Image	NPCR(%)	UACI(%)	Image	NPCR(%)	UACI(%)
Female	99.62	33.39	House	99.62	33.23	Couple	99.56	33.30
Tree	99.59	33.35	Beans	99.64	33.23	Splash	99.60	33.97

- (2) Key space. In order to resist a brute force attack, key space should be sufficiently large. For any cryptosystem key space represents the set of all possible keys required for encryption process. Generally, the size of key space should be greater than 2^{128} . In present scheme the parameters $a_1, b_1, a_2, b_2, a_3, \delta, L, S_P, t$ and p are used as secret keys, and we store each of them in 28 bits. So the key space of the proposed cryptosystem is 2^{280} which is larger than 2^{128} and hence capable to resist the brute force attack.
- (3) Known-plaintext/chosen-plaintext attack. In known-plaintext attack, the attacker has partial knowledge about the plain-image and cipher-image, and tries to break the cryptosystem, while in chosen-plaintext attack the attacker encrypts an arbitrary image to get the encryption keys. An all-white/black image is usually encrypted to test the performance of a scheme against these powerful attacks. We analysed our scheme by encrypting an all-white/black image of size 256×256 . The results are shown in Fig. 6 and Table 2, revealing that the encrypted images are significantly pseudo-randomised. Thus the proposed system is capable of preventing the above mentioned attacks.

Table 2. Security analysis of all-white/black encrypted images by the proposed encryption technique.

Plain-image	Entropy	Correlation of plain-image			NPCR(%)	UACI(%)
		Hori.	Diag.	Ver.		
All-white	7.9969	0.0027	0.0020	-0.0090	99.60	33.45
All-black	7.9969	-0.0080	0.0035	0.0057	99.62	33.41

5. Comparison and discussion

Apart from security analyses, the proposed scheme is compared with some well known image encryption techniques. The gray scale images of Lena_{256×256} and Lena_{512×512} are encrypted using the presented method, and experimental results are listed in Table 3. It is deduced that our scheme generates

Table 3. Comparison of the proposed encryption scheme with several existing cryptosystems for image Lena $_{m \times m}$, $m = 256, 512$.

Size m	Algorithm	Entropy	Correlation			NPCR (%)	UACI(%)	# S-boxes	Dynamic S-boxes
			Hori.	Diag.	Ver.				
256	Ours	7.9974	0.0001	-0.0007	-0.0001	99.91	33.27	1	Yes
	Ref. [25]	7.9993	0.0012	0.0003	0.0010	99.60	33.50	1	Yes
	Ref. [3]	7.9973	-	-	-	99.50	33.30	0	-
	Ref. [21]	7.9046	0.0164	-0.0098	0.0324	98.92	32.79	>1<50	Yes
	Ref. [20]	7.9963	-0.0048	-0.0045	-0.0112	99.62	33.70	8	Yes
	Ref. [37]	7.9912	-0.0001	0.0091	0.0089	100	33.47	0	-
	Ref. [38]	7.9974	0.0020	0.0020	0.0105	99.59	33.52	0	-
512	Ours	7.9993	0.0001	0.0042	0.0021	99.61	33.36	1	Yes
	Ref. [19]	7.9992	0.0075	0.0016	0.0057	99.61	33.38	1	No
	Ref. [23]	7.9993	-0.0004	-0.0018	0.0001	99.60	33.48	1	No
-	Ref. [39]	7.9970	-0.0029	0.0135	0.0126	99.60	33.48	0	-
	Ref. [40]	7.9994	0.0018	-0.0012	0.0011	99.62	33.44	>1	Yes
	Ref. [2]	7.9993	0.0032	0.0011	-0.0002	99.60	33.47	>1	Yes

cipher-images with comparable security. Furthermore, we remark that the scheme in [23] generates pseudo-random numbers using group law on EC, while the proposed method generates pseudo-random numbers by constructing triads using auxiliary parameters of elliptic surfaces. Group law consists of many operations, which makes the pseudo-random number generation process slower than the one we present here. Moreover, the S-box used in [23] is a static one which is vulnerable [41], while our scheme generates a dynamic S-box for each image which is more secure [42]. The scheme in [20] decomposes an image to eight blocks and uses eight dynamic S-boxes for encryption purpose. The computation of multiple S-boxes takes more time than computing only one S-box. Similarly the techniques in [2,21] use a set of S-boxes and encrypt an image in blocks, while our newly developed scheme encrypts the whole image using only one dynamic S-box. Thus, our scheme is faster than the schemes in [2,21]. The security system in [39] uses a chaotic system to encrypt blocks of an image. The results in Table 3 reveal that our proposed system is cryptographically stronger than the scheme in [39]. The algorithms in [3,37] combine chaotic systems and different ECs to encrypt images. It follows from Table 3 that the security level of our scheme is comparable to that of the schemes in [3,37]. The technique in [38] uses double chaos along with DNA coding to get good results as shown in Table 3, but the results obtained by the new scheme are better than that of [38]. Similarly the technique in [25] encrypts images using ECs, the disadvantage of that scheme is that it does not generate an S-box for each input image and the generation of an S-box needs trials, while our scheme generates a dynamic S-box for each input image, thus making our scheme faster and more robust than the scheme developed in [25].

6. Conclusion

An image encryption scheme based on quasi-resonant triads and MECs is introduced. The proposed technique constructs triads to generate pseudo-random numbers and computes a MEC to construct an S-box for each input image. The pseudo-random numbers and S-box are then used for altering and scrambling the pixels of the plain-image respectively. As for the advantages of our proposed method, firstly triads are based on auxiliary parameters of elliptic surfaces, and thus pseudo-random numbers and S-boxes generated by our method are highly sensitive to the plain-image, which prevents adversaries from initiating any successful attack. Secondly, generation of triads using auxiliary parameters of elliptic surfaces consumes less time than computing points on ECs (we find a 4x speed increase for a range of image resolutions $m \in [128, 512]$), which makes the new encryption system relatively faster. Thirdly, our algorithm generates the cipher-images with an appropriate security level.

In summary, all of the above analyses imply that the presented scheme is able to resist all attacks. It has high encryption efficiency and less time complexity than some of the existing techniques. In the future, the current scheme will be further optimised by means of new ideas to construct the S-boxes using the constructed triads, so that for each input image we will not need to compute a MEC.

Author Contributions: All authors contributed equally to this work.

Funding: This research is funded through HEC project NRPU-7433.

Acknowledgments: We thank Gene Kopp for useful comments and suggestions.

Conflicts of Interest: The authors declare no conflict of interest. The funding sponsors had no role in the design of the study; in the collection, analyses, or interpretation of data; in the writing of the manuscript, and in the decision to publish the results.

Abbreviations

The following abbreviations are used in this manuscript:

MEC	Mordell elliptic curve
S-box	Substitution box
EC	Elliptic curves

References

1. Mahmud, M., Lee, M., and Choi, J. Y. Evolutionary-Based Image Encryption using RNA Codons Truth Table. *Optics and Laser Technology* **2020**, *121*, 105818 (1-8).
2. Zhang, X., Mao, Y., and Zhao, Z. An Efficient Chaotic Image Encryption Based on Alternate Circular S-boxes. *Nonlinear Dynamics* **2014**, *78(1)*, 359-369.
3. El-Latif, A. A. A., and Niu, X. A Hybrid Chaotic System and Cyclic Elliptic Curve for Image Encryption. *AEU-International Journal of Electronics and Communications* **2013**, *67(2)*, 136-143.
4. Yang, Y. G., Pan, Q. X., Sun, S. J., and Xu, P. Novel Image Encryption Based on Quantum Walks. *Scientific Reports* **2015**, *5(1)*, 1-9.
5. Zhong, H., Chen, X., and Tian, Q. An Improved Reversible Image Transformation Using K-Means Clustering and Block Patching. *Information* **2019**, *10(1)*, 1-17.
6. Li, C., Lin, D., and Lü, J. Cryptanalyzing an Image-Scrambling Encryption Algorithm of Pixel Bits. *IEEE MultiMedia* **2017**, *24(3)*, 64-71.
7. Hua, Z., Yi, S., and Zhou, Y. Medical Image Encryption using High-Speed Scrambling and Pixel Adaptive Diffusion. *Signal Processing* **2018**, *144*, 134-144.
8. Xie, E. Y., Li, C., Yu, S., and Lü, J. On the Cryptanalysis of Fridrich's Chaotic Image Encryption Scheme. *Signal processing* **2017**, *132*, 150-154.
9. Alzaidi, A. A., Ahmad, M., Ahmed, H. S., and Solami, E. A. Sine-Cosine Optimization-Based Bijective Substitution-Boxes Construction using Enhanced Dynamics of Chaotic Map. *Complexity* **2018**, 1-16.
10. Azam, N. A. A Novel Fuzzy Encryption Technique Based on Multiple Right Translated AES Gray S-Boxes and Phase Embedding. *Security and Communication Networks* **2017**, 1-10.
11. Luo, Y., Tang, S., Qin, X., Cao, L., Jiang, F., and Liu, J. A Double-Image Encryption Scheme Based on Amplitude-Phase Encoding and Discrete Complex Random Transformation. *IEEE Access* **2018**, *6*, 77740-77753.
12. Li, J., Li, J. S., Pan, Y. Y., and Li, R. Compressive Optical Image Encryption. *Scientific Reports* **2015**, *5*, 1-10.
13. Ismail, S. M., Said, L. A., Radwan, A. G., Madian, A. H., and Abu-ElYazeed, M. F. A Novel Image Encryption System Merging Fractional-Order Edge Detection and Generalized Chaotic Maps. *Signal Processing* **2020**, *167*, 107280 (1-21).
14. Tang, Z., Yang, Y., Xu, S., Yu, C., and Zhang, X. Image Encryption with Double Spiral Scans and Chaotic Maps. *Security and Communication Networks* **2019**, 1-16.

15. Abdelfatah, R. I. Secure Image Transmission Using Chaotic-Enhanced Elliptic Curve Cryptography. *IEEE Access* **2019**, 1-16.
16. Yu, J., Guo, S., Song, X., Xie, Y., and Wang, E. Image Parallel Encryption Technology Based on Sequence Generator and Chaotic Measurement Matrix. *Entropy* **2020**, *22*(1), 1-16.
17. Zhu, S., Zhu, C., and Wang, W. A Novel Image Compression-Encryption Scheme Based on Chaos and Compression Sensing. *IEEE Access* **2018**, *6*, 67095-67107.
18. ElKamchouchi, D. H., Mohamed, H. G., and Moussa, K. H. A Bijective Image Encryption System Based on Hybrid Chaotic Map Diffusion and DNA Confusion. *Entropy* **2020**, *22*(2), 1-18.
19. Cheng, P., Yang, H., Wei, P., and Zhang, W. A Fast Image Encryption Algorithm Based on Chaotic Map and Lookup Table. *Nonlinear Dynamics* **2015**, *79*(3), 2121-2131.
20. Belazi, A., El-Latif, A. A. A., and Belghith, S. A Novel Image Encryption Scheme Based on Substitution-Permutation Network and Chaos. *Signal Processing* **2016**, *128*, 155-170.
21. Rehman, A. U., Khan, J. S., Ahmad, J., and Hwang, S. O. A New Image Encryption Scheme Based on Dynamic S-boxes and Chaotic Maps. *3D Research* **2016**, *7*(1), 1-8.
22. Jia, N., Liu, S., Ding, Q., Wu, S., and Pan, X. A New Method of Encryption Algorithm Based on Chaos and ECC. *Journal of Information Hiding and Multimedia Signal Processing* **2016**, *7*(3), 637-643.
23. Toughi, S., Fathi, M. H., and Sekhavat, Y. A. An Image Encryption Scheme Based on Elliptic Curve Pseudo Random and Advanced Encryption System. *Signal processing* **2017**, *141*, 217-227.
24. Liu, H., and Liu, Y. (2014). Cryptanalyzing an Image Encryption Scheme Based on Hybrid Chaotic System and Cyclic Elliptic Curve. *Optics & Laser Technology* **2014**, *56*, 15-19.
25. Hayat, U., and Azam, N. A. A Novel Image Encryption Scheme Based on an Elliptic Curve. *Signal Processing* **2019**, *155*, 391-402.
26. Bustamante, M. D., and Hayat, U. Complete Classification of Discrete Resonant Rossby/Drift Wave Triads on Periodic Domains. *Communications in Nonlinear Science and Numerical Simulation* **2013**, *18*(9), 2402-2419.
27. Hayat, U., Amanullah, S., Walsh, S., Abdullah, M., and Bustamante, M. D. Discrete Resonant Rossby/Drift Wave Triads: Explicit Parameterisations and a Fast Direct Numerical Search Algorithm. *Communications in Nonlinear Science and Numerical Simulation* **2019**, *79*, 104896 (1-19).
28. Azam, N. A., Hayat, U., and Ullah, I. Efficient Construction of S-boxes Based on a Mordell Elliptic Curve Over a Finite Field. *Frontiers of Information Technology and Electronic Engineering* **2019**, *20*(10), 1378-1389.
29. Azam, N. A., Hayat, U., and Ullah, I. An Injective S-Box Design Scheme over an Ordered Isomorphic Elliptic Curve and Its Characterization. *Security and Communication Networks* **2018**, 1-9.
30. Charney, J. G. On the scale of atmospheric motions. *Geophys. Public* **1948**, *17*, 3-17.
31. Hasegawa, A. and Mima, K. Pseudo-three-dimensional turbulence in magnetized nonuniform plasma. *The Physics of Fluids* **1978**, *21*(1), 87-92.
32. Connaughton, C.P., Nadiga, B.T., Nazarenko, S.V., and Quinn, B.E. Modulational instability of Rossby and drift waves and generation of zonal jets. *Journal of Fluid Mechanics* **2010**, *654*, 207-231.
33. Harris, J., Connaughton, C., and Bustamante, M.D. Percolation transition in the kinematics of nonlinear resonance broadening in Charney-Hasegawa-Mima model of Rossby wave turbulence. *New Journal of Physics* **2013**, *15*(8), 083011.
34. Galperin, B. and Read, P. L., editors. Zonal Jets: Phenomenology, Genesis, and Physics. *Cambridge University Press* **2019**.
35. Kopp, G. S. The Arithmetic Geometry of Resonant Rossby Wave Triads. *SIAM Journal on Applied Algebra and Geometry* **2017**, *1*(1), 352-373.
36. USC-SIPI Image Database available at <http://sipi.usc.edu/database/database.php>
37. Wu, J., Liao, X., and Yang, B. Color Image Encryption Based on Chaotic Systems and Elliptic Curve ElGamal Scheme. *Signal Processing* **2017**, *141*, 109-124.
38. Wan, Y., Gu, S., and Du, B. A New Image Encryption Algorithm Based on Composite Chaos and Hyperchaos Combined with DNA Coding. *Entropy* **2020**, *22*(2), 1-19.

39. Tong, X. J., Zhang, M., Wang, Z., and Ma, J. A Joint Color Image Encryption and Compression Scheme Based on Hyper-Chaotic System. *Nonlinear Dynamics* **2016**, *84(4)*, 2333-2356.
40. Zhang, Y., and Xiao, D. An Image Encryption Scheme Based on Rotation Matrix Bit-Level Permutation and Block Diffusion. *Communications in Nonlinear Science and Numerical Simulation* **2014**, *19(1)*, 74-82.
41. Rosenthal, J. A Polynomial Description of the Rijndael Advanced Encryption Standard. *Journal of Algebra and its Applications* **2003**, *2(2)*, 223-236.
42. Kazlauskas K, Kazlauskas J. Key-Dependent S-box Generation in AES Block Cipher system. *Informatica* **2009**, *20(1)*, 23-34.